

CAREER: A new phase field based fracture mechanics theory for understanding the origin of toughness enhancement in bio-inspired materials with intricate 3D interfaces

1 Introduction

Background and open research questions In most engineering materials, from steels to ceramics, strength and toughness are mutually exclusive. That is, there are few materials that are both strong and tough [1]. The PI believes that this is a critical bottleneck for aerospace, transportation, and energy production technologies. Recently, however, it has been shown that some structural biomaterials (SBs) possess both high strength and high toughness [2–10]. In many cases, SBs are heterogeneous, and consist of a ceramic and an organic phase mixed together in intricate 3D patterns over a range of length scales [11, 12]. The way that these two phases are interlaced, which we refer to as the SB's architecture, is extremely complex compared to architectures typically seen in engineering composites, such as ceramic matrix composites [13, 14]. Some examples of architectures seen in SBs are the brick-and-mortar arrangement of ceramic tablets in shells [15–17], and the interlocking helices in the club-like appendage of the mantis shrimp [18–20]. Since these SBs are characterized by the numerous, intricately arranged, interfaces between the ceramic phases, we refer to them as interface dense SBs, or *id*-SBs.

While *id*-SBs are often composed of >95% brittle ceramic material by volume, they have been shown to possess extraordinary toughness properties while being able to maintain both strength and stiffness [4, 21–23]. For example, the total energy dissipated during the fracture of nacre has been shown to exceed that of its constituent ceramic material, aragonite, by three orders of magnitude [18, 19]. Such toughness enhancement is also observed in a number of other *id*-SBs, such as bone and dentin [6, 24–26]. This is a very intriguing effect since it cannot be explained using standard composite mechanics ideas, such as the rule of mixtures (see Figure 1 (b)) [27]. The apparent correlation between the SBs' intricate architectures and their extraordinary mechanical properties has motivated many studies that investigate this connection [8, 21, 22, 28–34]. We believe that the key questions in this line of investigation are: (Q.1) Are specific architectural motifs the key to overcoming the tradeoff between strength and toughness? (Q.2) Or is the mechanical behavior of the interfaces actually more important than architectural motifs? (Q.3) If specific architectural motifs are the key, then what are they and what are the mechanisms through which they enhance toughness? (Q.4) Is there an upper bound to the potential toughness enhancement? (Q.5) Is it critical that the architecture be spread over several length scales, i.e., is hierarchy always important? Currently, there are no satisfactory answers to these questions.

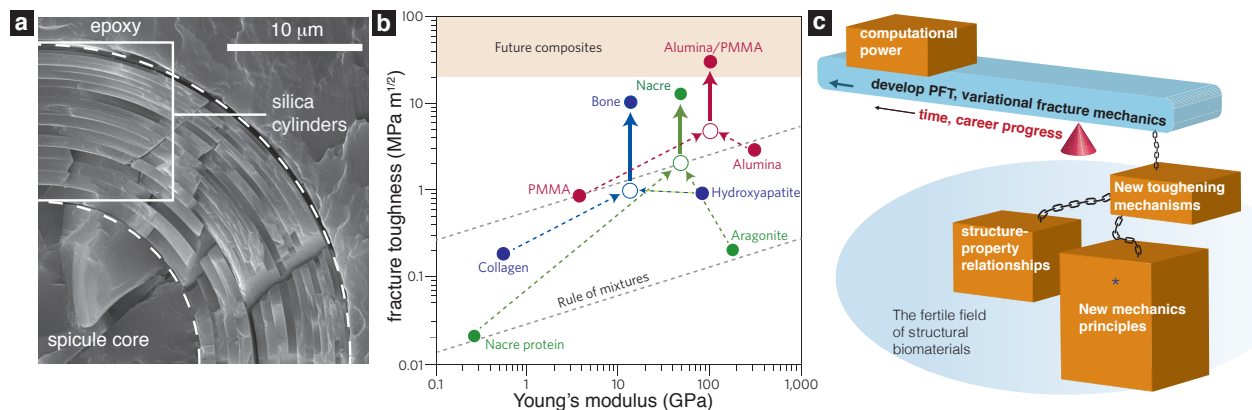


Figure 1: Motivation for the proposed effort. (a) A SEM image of a *E. aspergillum* spicule's cross-section. The spicule's architecture consists of a concentric assembly of roughly 25 silica cylinders and a monolithic silica core. (b) The toughnesses of many SBs exceed that of their constituent materials. The extent to which toughness is enhanced cannot be predicted by the rule of mixtures. Bio-inspired composites, such as brick-and-mortar Alumina/PMMA composites, produce similar deviations from the rule of mixtures' predictions (reprinted from [27]). (c) The PI's career plan to develop new variational fracture mechanics theories and leverage them to discover new toughening mechanisms and new mechanics principles.

Overarching objective and its key hurdles The PI's overarching career objective is to answer the questions Q.1–5. Through the proposed project the PI plans to pursue his overarching career objective by addressing a key issue that is critical for answering Q.1–5. This key issue is the lack of a strategy for identifying which architectural parameters are the most important for toughness enhancement in a given *id*-SB. Architectures of important *id*-SBs, such as bone and conch shell (*strombus gigas*), possess at least several dozen architectural parameters. Due to this complexity, it is seldom clear which features are important and should therefore be included in a model. Typical models aimed at explaining toughness enhancement focus on a small subset of the *id*-SBs' architectural motifs and also make a number of simplifying assumptions regarding the deformation behavior of the materials and the interfaces. Naturally, by focusing on different architectural subsets and using different simplifying assumptions one can come up with a number of models. Since it is not possible to simply "see" inside the material and check whether the mechanisms presumed in the models are truly active, it is difficult to determine the validity of any of the typical models. Comparing the models with experiments and making self consistency checks does help to reduce the number of plausible models. However, even after such checks a considerable number of plausible models can remain. For example, there are over five models that are actively discussed in the community for explaining the toughness enhancement in nacre [35–40]. Generally, there is no consensus as to which of the several plausible models is the most correct. In fact, it is also fair to question if any of the proposed models are correct. This is because the typical models are based on what are termed "intrinsic" and "extrinsic" toughening mechanisms that were originally put forward for explaining toughness enhancement in synthetic ceramic composites, which of course, are far simpler in architectural complexity than *id*-materials. Furthermore, the "intrinsic" and "extrinsic" mechanisms such as crack bridging, frictional pull-out of fibers or lamellae, or plastic dissipation at the interfaces caused by failure of sacrificial bonds [41] only capture a portion of the toughness enhancement that is experimentally observed in *id*-SBs [2, 3, 18, 42].

Scientific vision for achievement of the overarching research objective The PI proposes to address the key issue by developing a new phase field-based fracture mechanics theory (PFT) that would enable accurate and robust computer simulation of the *id*-materials' failure behaviors. The simulations would retain the full complexity of the *id*-materials' architectures and include only a minimal number of simplifying assumptions. We envision the PFT computational tools being used in the following way. Consider an *id*-SB that displays exceptional toughness in a fracture test. We would begin by building a family of computer aided design (CAD) models that incorporate different subsets of the material's architectural features. We would then perform virtual mechanical tests on those CAD models using the PFT tools. Small-scale material parameters, such as interface toughness and strength, that are difficult to measure experimentally will be used as fitting parameters in the PFT computations to get their predictions to match the measurements as closely as possible. These predictions will be used to identify the smallest subset of architectural features that are responsible for the majority of the SB's toughness. An applied mechanics type model will then be built by incorporating only that smallest subset. The virtual tests will be further analyzed to identify the key mechanisms responsible for the SB's toughness. That knowledge will be used to guide the development of the applied mechanics model.

Hypothesis underlying the proposed research The proposed development of the PFT is crucial in order to be able to accurately and robustly simulate the failure behavior of *id*-materials. We hypothesize that the toughness enhancement in *id*-SBs is due to the interfaces acting as traps and mazes. The stiff phases fail through brittle fracture. However, the cracks emanating from the brittle region inevitably encounter the interfaces, as the interfaces are densely distributed. The interfaces trap the cracks and make them consume much more energy to spread across the specimen. They do this primarily by pinning, deflecting, and splitting the cracks [43–45]. Our hypothesis is motivated by experimental observations of dense crack patterns in failed *id*-materials [3, 46], our preliminary results, and most importantly the PI's previous research on contact interface toughening caused by surface architectures [47–49].

Robust and accurate simulation of the creation and evolution of complex crack patterns at the scale of complexity seen in *id*-SBs is a viable idea only through the use of PFT computational tools. The crack patterns seen during the failure of *id*-SBs are simply too complex for standard fracture simulation tools, such as element deletion methods [50, 51], singularity element methods [52–54], cohesive zone method (CZM) [55, 56] and even extended finite element method (XFEM) [57–60]. These standard tools are based on the clas-

sical version of fracture, which is notorious for causing numerical difficulties due to the presence of stress singularities. Numerical convergence problems [61], mesh sensitivity [59, 61], need of *a priori* knowledge of topology changes (crack branching, merging, and nucleation) [61], ill-conditioning issues [62], and need of special treatment for modeling intersecting and branching cracks—which is prohibitively complicated in 3D—make standard fracture simulation tools ill-suited for performing virtual experiments on realistic *id*-SB models. In contrast, PFT is an alternate theory of brittle fracture in which complex crack patterns are represented through a scalar-valued field, often termed the damage field, and which does not contain any stress singularities. The technical details of PFT are discussed in §2. The representation of the cracks as a scalar field dramatically reduces the computational and numerical challenges and makes it straightforward to simulate the highly complex crack patterns seen in *id*-SBs.

Specific research objectives The PFT we focus on originated in the pure mathematics community. The PFT tools' terrific computational and numerical advantages are a result of its extremely strong mathematical foundation. However, it was formulated with a minimal inclusion of mechanics and physics principles. For that reason in many instances PFT predicts unphysical behaviors. We have identified the most important of these behaviors to be crack broadening. Furthermore, it is only possible to model bulk fracture, and not interfacial fracture with the current PFT. Thus, the first specific research objective of our proposal (**Sro.I**) is to resolve the key problem of broadening in PFT and introduce the capability to model interfacial fracture.

Mechanism to assess success: The success of the project will be assessed through the completion of *Sro.II* and *Sro.III*, which we describe below. If PFT tools are to function as investigative tools for identifying the key architectural features in *id*-SBs, as described in the scientific vision, then it is important that they are able to reproduce the salient features of the experimentally observed failure response of *id*-SBs. Therefore, our second research objective (**Sro.II**) is to evaluate the potential of the newly developed PFT in predicting the failure behavior of an *id*-SB. The last part of the PI's scientific vision is that the PFT computational tools will help in identifying and understanding the mechanisms through which a particular architectural motif enhances a SB's toughness. Through that understanding, the tools will guide the development of applied mechanics models that efficiently capture these mechanisms. Therefore, our final specific research objective for this project (**Sro.III**) is to apply the developed PFT computational tools to understand the mechanism through which a prototypical SB architectural motif (wavy-interface) enhances toughness and develop an applied mechanics model that will capture that mechanism.

The research objectives are discussed in §2–4. In each section we explain the challenges that must be overcome to achieve the specific research objective. Following that, we outline our strategy and the tasks we plan to carry out to overcome these challenges. The results from the preliminary research conducted in preparation for this proposal are distributed across these three sections. We use them to illustrate the challenges and their proposed resolution. The relationship between the proposed research and the past and current research of the PI and other research groups is also distributed across these three sections.

1.1 Intellectual merit and Long term career objective

Answering Q.1–5 is a prerequisite for creating a systematic strategy for reproducing the exceptional toughness of *id*-SBs in bio-inspired *id*-materials. However, addressing these questions is actually more important for the purpose of advancing fundamental science. The new PFT will allow one to observe the mechanisms and phenomena that take place inside an *id*-material as it fails. We believe that this will invariably lead to the discovery of fundamental knowledge of deep scientific value in the field of mechanics of materials. We elaborate on this using an historical example. Galileo observed that the bones of smaller animals are more slender than those of larger animals [63]. This led him to deducing that load divided by the cross-sectional area is the critical quantity that dictates the largest load a structure can transmit without failing. By observing the phenomena of size scaling Galileo arrived at a primitive version of the stress-based failure criteria. Thus, by allowing one to “observe” new phenomena inside a material the new PFT tools will bring new mechanics principles to light. The fact that Q.1–5 remain unanswered implies that SBs hide a wealth of undiscovered material toughening mechanisms, and consequently many new mechanics principles, within them.

Our research involving PFT is directed in an exceptionally promising direction. Understanding the mechanics and physics of fracture is of great scientific and engineering importance. The current PFT is an alternate,

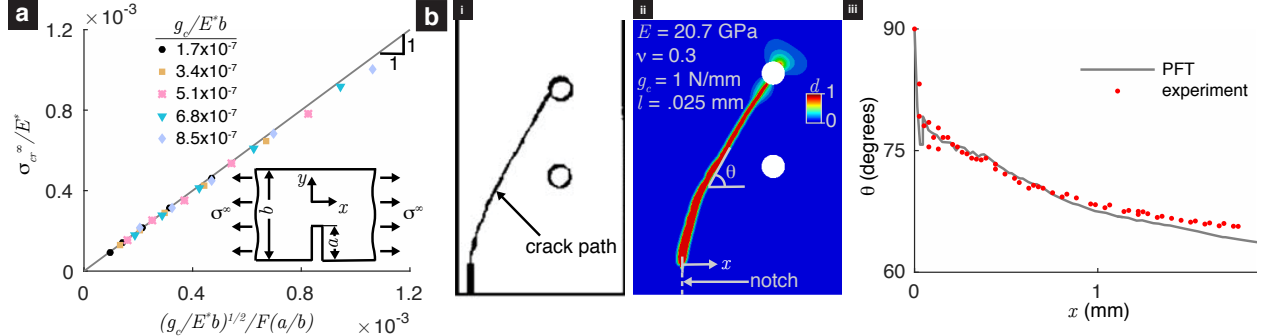


Figure 2: Comparison of PFT predictions with LEFM and experiments. (a) Edge-notched geometry subjected to a far-field stress σ_∞ . The dimensionless stress at which the crack initiates $\sigma_{cr}/\sigma_\infty$ as a function of dimensionless variables, g_c/E^*b and a/b obtained from the analytical solution. For different values of g_c/E^*b , the markers lie close to the reference line shown in gray within an error of 5%. (b) Comparison of PFT predictions with an edge notch three-point bending test in which the sample has three holes drilled in it. (i) The experimentally measured crack path from [66]. (ii) Contour of the damage field d , where $d = 1$ is indicated by red contour level signifying the location of the crack. (iii) Comparison of the measured crack path and the PFT predictions using the crack angle, θ shown in (ii).

and in a sense approximate, model of brittle fracture. So, exciting future directions could be about how one would extend PFT to model more complicated, and equally more important, cases of quasi-brittle and ductile fracture. There are currently attempts to extend PFT to ductile fracture [64, 65]. However, most of such approaches so far have been *ad hoc* in nature. With brittle fracture being the most simple of cases, one would have to first develop a physically valid PFT model of brittle fracture before they can hope to develop a physically valid PFT model of quasi-brittle or ductile fracture. However, as is the topic of this proposal, even when attempting to model just brittle fracture the PFT displays a number of shortcomings. The most important of these, of course, is broadening, which we plan on rectifying by carrying out this project. Considering the remarkable impact it can have, one of the PI's long term career objectives is to develop a physically valid PFT model that is based on a strong mechanics foundation and that can predictively model a number of complex effects, such as ductile fracture, plasticity, etc., simultaneously (see Figure 1 (c)). Therefore, carrying out this project is an important and mandatory first step for the PI is his pursuit of this long term career objective.

2 *Sro.I.: Resolve the key problem of broadening in PFT and introduce the capability to model interfacial fracture*

2.1 Technical details and introduction of the PFT

Different versions of PFT can be found in literature [67, 68]. In our work we will focus on the PFT theory presented by Bourdin et al. [67, 69]. In the last three years we have experimented with different PFTs and found that Bourdin et al.'s PFT is the most suitable for analyzing engineering problems, since it can be generalized and extended in a straightforward manner to handle finite deformations, dynamics, different hyperelastic material models, and complicated geometries and loading programs. Furthermore, Bourdin et al.'s theory has a strong mathematical foundation. The theory's underlying mathematical results make it clear as to what physics the theory is aiming to approximate, and give a rigorous proof, using the notion of Γ -convergence [70], that the predictions of the theory will correctly capture that physics [71, 72].

The physics underlying Bourdin et al.'s PFT is the variational fracture theory (VFT) put forward by Marigo and Francfort [73]. The VFT is a generalization of the configurational force balance ideas put forward by Griffith [74]. Griffith postulated that for a crack to grow the energy release rate should be equal to or exceed the fracture toughness of the material. The VFT generalizes this idea by postulating that on the application of a load increment, the observed crack pattern is the one which minimizes the total energy of the system over all admissible crack patterns. The admissible crack patterns are defined to be those that contain the crack pattern from the previous load increment as a subset. This constraint introduces irreversibility and history dependence into the problem.

In the absence of body forces, the total energy, E , can be written as the surface energy and what we define to be the equilibrium strain energy. The surface energy is $\int_{\Gamma} g_c d\Gamma$, where Γ is the crack pattern and g_c is the material's fracture toughness. The strain energy for a hyperelastic solid can be written as $\int_{B_0 \setminus \Gamma} \Psi_0(\mathbf{X}, \mathbf{C}) d\Omega$, where Ψ_0 is the strain energy density, and \mathbf{X} is a material point in the solid's reference configuration B_0 . The tensor $\mathbf{C} := \mathbf{F}^T \mathbf{F}$ is the right Cauchy-Green deformation tensor, where $\mathbf{F} = \nabla_0 \mathbf{u} + \mathbf{I}$ is the deformation gradient, \mathbf{u} is the displacement vector, \mathbf{I} is the identity tensor, and $\nabla_0(\cdot)$ is the gradient operator defined with respect to \mathbf{X} . The equilibrium strain energy is then defined as the infimum value of the strain energy computed over the set of all admissible displacement fields. Note that the equilibrium strain energy term is a volume (resp. area) integral, whereas the surface energy term is a surface (resp. line) integral in 3D (resp. 2D). This makes it very difficult to solve the variational problem of finding the new crack pattern that minimizes the total energy after a load increment. To circumvent this problem, Bourdin et al. [69] introduced the following regularized or "smoothed" energy functional,

$$E_\ell(\mathbf{u}, d) := \int_{B_0} \Psi_d(\mathbf{X}, \mathbf{C}, d) d\Omega + g_c/2 \int_{B_0} (d(\mathbf{X})^2/\ell + \ell \|\nabla_0 d(\mathbf{X})\|^2) d\Omega, \quad (1)$$

where $\|\cdot\|$ is the Euclidean 2-norm, the parameter ℓ has units of length and is called the regularization parameter, $\Psi_d(\mathbf{X}, \mathbf{C}, d) = (1 - d)^2 \Psi_0(\mathbf{X}, \mathbf{C})$ is called the degraded strain energy density, and we call $d(\mathbf{X})$ the damage field, which takes values between zero and unity. By construction, as d increases the material's capacity to store elastic energy degrades. Therefore, d can be interpreted as a measure of damage. When $d = 0$ the material point is completely undamaged, and when $d = 1$ the material point has lost all capacity to store strain energy. The crack pattern region, Ω_c , is now defined to be a path connected subset of the solid B_0 such that $d(\mathbf{X}) \geq c$, $\forall \mathbf{X} \in \Omega_c$, where c is a real number just smaller than unity, and the set $\{\mathbf{x} \in \Omega_c : d(\mathbf{X}) = 1\}$ is non-empty. Since all integrals in the functional E_ℓ are now over B_0 , we can attempt to minimize E_ℓ with respect to (\mathbf{u}, d) by solving its corresponding Euler-Lagrange equations (for details see [75]).

If $(\mathbf{u}_\ell^*, d_\ell^*)$ are smooth minimizers of E_ℓ then it is necessary that they satisfy the Euler-Lagrange equations corresponding to E_ℓ , which are,

$$\nabla_0 \cdot \mathbf{P} = 0, \quad \text{and} \quad g_c \ell \nabla_0 \cdot (\nabla_0 d) - g_c d/l = \partial \Psi_d / \partial d, \quad (2)$$

for all $\mathbf{X} \in B_0$, where \mathbf{P} is the first Piola-Kirchhoff stress tensor, which in the present case comes out to be equal to $(1 - d)^2 \partial \Psi_0 / \partial \mathbf{F}$. The governing equations, Eqns. (2), are solved along with the standard displacement and traction boundary conditions, and the new boundary condition that the component of $\nabla_0 d$ normal to the solid's boundary vanish. For ease of elaboration, in deriving Eqns. (2) we ignored the irreversibility/history-dependence constraint. See [76] for a version of the governing equations for (\mathbf{u}, d) that respects the irreversibility constraint. As per the aforementioned Γ -convergence result, the crack region Ω_c^* that corresponds to the minimizer $(\mathbf{u}_\ell^*, d_\ell^*)$ converges to the crack path postulated by the VFT as $\ell \rightarrow 0$.

As preliminary research, we implemented non-linear finite element techniques [77] to numerically solve the PFT Eqns. (2) using the algorithms presented in [75]. The results of these calculations are shown in Figures 2–5. These results were generated for the special case of small deformations and Ψ_0 corresponding to the strain energy density of a homogenous, isotropic, linear elastic material model. We found that in many important cases the results of the PFT match the predictions of linear elastic fracture mechanics (LEFM), see, e.g., Figure 2 (a). It has also been shown that the crack path predicted by the PFT matches the crack path seen in many experiments [75, 76, 78]. We were also able to reproduce these results, e.g., see Figure 2 (b).

However, we also found a number of cases in which the PFT predicted unphysical effects. We consider here the most important of such effects, which we have termed *Broadening*.

2.2 Key challenges for Sro./

Broadening A crack by definition has zero thickness. Almost all continuum mechanics fracture theories model cracks as curves or surfaces in the reference configuration. Similarly, some of the most important computational fracture mechanics models, such as XFEM and CZM, also model the cracks as having zero

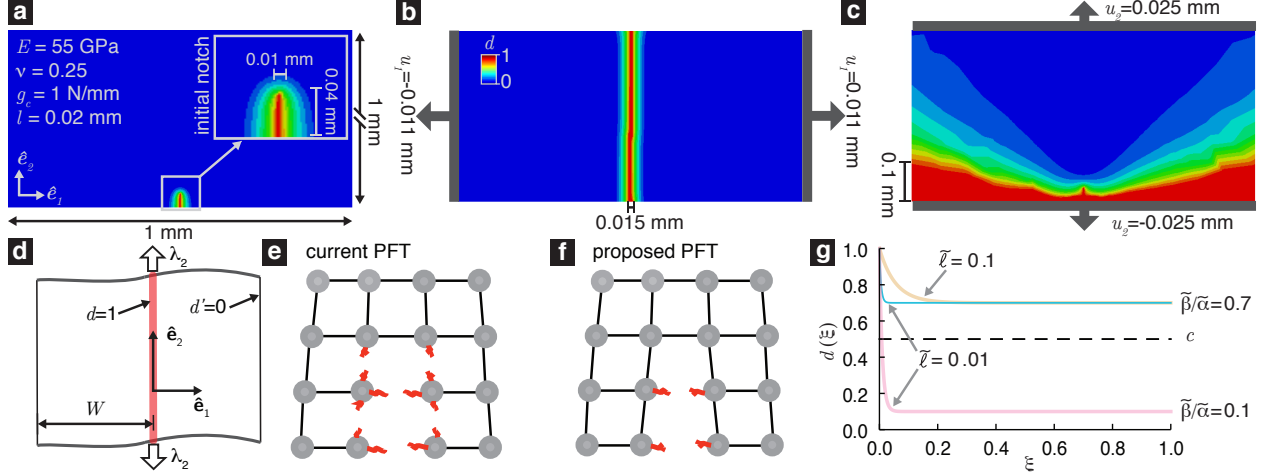


Figure 3: Example simulations demonstrating the problem of broadening. (a) Experiment geometry and problem parameters. Only the lower half of the plate in the $\hat{\mathbf{e}}_2$ direction is shown since $d \approx 0$ in the upper half for (a)–(c). The notch is not explicitly incorporated as part of the plate's geometry but rather is represented as a small region where $d = 1$, as shown in the inset. (b) The plate in (a) is loaded in uniaxial tension by displacing the boundaries marked in gray in the $\pm\hat{\mathbf{e}}_1$ direction. A crack (the red contour level) propagates from the notch in the $\hat{\mathbf{e}}_2$ direction until the plate is cleaved into two pieces. The crack's thickness is roughly equal to ℓ . (c) The plate in (a) is loaded in uniaxial tension parallel to the notch direction by displacing the boundaries marked in gray in the $\pm\hat{\mathbf{e}}_2$ direction. Damage progresses from the notch in the $\pm\hat{\mathbf{e}}_1$ directions until there is a region of completely disintegrated material (i.e., $d \approx 1$) spanning the entire width of the plate. The thickness of this region is much larger than ℓ . (d) A 2D strip with infinite length in the $\hat{\mathbf{e}}_2$ direction stretched parallel to a crack (shown in red) along its length. (g) The variation of the damage, d , over the half-width of the 2D cracked strip shown in (d). The variable $\xi = x/W$, and x is the Cartesian coordinate in the $\hat{\mathbf{e}}_1$ direction shown in (d).

thickness [79, 80]. In contrast, a very conspicuous feature of the PFT is that in it the crack thickness is non-zero. Recall from §2 that in PFT the crack is defined as the region Ω_c , which has the same dimensionality as the solid \mathcal{B}_0 .

The fact that the crack thickness is non-zero in PFT does not preclude PFT from being a useful and predictive theory of fracture. For instance, consider again the remarkable match of the PFT's predictions with LEFM and experimental results shown in Figure 2. However, for the cracks in the PFT theory to be physically meaningful it is critical that their thicknesses be much smaller than the physical dimensions of the solid. This is because in the PFT the crack region Ω_c has zero stiffness. Thus, if a crack thickness is not much smaller than the solid's dimensions then the situation resembles that of a solid undergoing plastic failure rather than brittle fracture. It is generally argued that the thickness of the crack is of the order ℓ , the regularization parameter [81]. And hence by choosing ℓ to be much smaller than the characteristic dimension of the solid, W , i.e., $\ell/W \ll 1$, one can ensure that the results are always meaningful, i.e., the failure has the physical features of brittle fracture. However, in some test cases we observed that the crack thickness was comparable to the dimensions of the solid even though ℓ was much smaller than the solid's dimensions. We termed this effect *broadening*. Example test cases displaying broadening are shown in Figure 3.

We found that the broadening effect was not due to human errors or numerical artifacts, but due to the inadequacy of the condition $\ell/W \ll 1$. This fact is best illustrated by the following analytical solution to the governing Eqns. (2) for a simple boundary value problem.

Consider a 2D strip of infinite length and width $2W$ that is shown in Figure 3 (d). The strip is composed of an incompressible neo-Hookean material so that the degraded strain energy density in this case is $(1 - d)^2(\mu/2)(\lambda_1^2 + \lambda_2^2 - 2)$. The strip has a pre-existing crack along its length (shown in red in Figure 3 (d)). Starting from this state, the strip is uniformly stretched with a stretch ratio of λ_2 in the crack direction (marked as $\hat{\mathbf{e}}_2$ in Figure 3 (d)). Let $\tilde{\beta} := \mu(\lambda_2^2 + 1/\lambda_2^2 - 2)W^2/g_c\ell$ be a dimensionless measure of this straining, where μ is the shear modulus, and let $\tilde{\alpha} := \tilde{\beta} + 1/\tilde{\ell}^2$, where $\tilde{\ell} := \ell/W$. Assuming that the solution does not vary along the strip's length, an analytical solution for the damage field can be obtained for this problem. It can be shown using the analytical solution that in the majority of the strip the damage variable is approximately equal to $\tilde{\beta}/\tilde{\alpha}$, see Figure 3 (g). If $\tilde{\beta}/\tilde{\alpha}$ becomes greater than c , which, recall, is the parameter

used for defining the crack region Ω_c , then the crack width will become equal to the strip's width. That is, there will be broadening. And this would occur irrespective of how small ℓ is as long as $\tilde{\beta}/\tilde{\alpha}$ is greater than c , see Figure 3 (g). Therefore in order to prevent broadening, it is also necessary that $\tilde{\beta}/\tilde{\alpha}$ is much smaller than unity, which in terms of dimensional variables reads $\ell \ll \ell_c$, where $\ell_c := g_c/\mu(\lambda_2^2 + 1/\lambda_2^2 - 2)$ is a length scale characteristic of the material and loading. In summary, when the material and the loading are such that $\ell_c \ll W$, the condition $\ell \ll W$ alone is not sufficient to prevent broadening.

Our preliminary research also has the following important consequence. In view of broadening, current PFT cannot be used as the basis for developing practical investigative tools. As per the Γ convergence proof mentioned in §2 the solution to the Eqns. (2) becomes meaningful only in the limit $\ell \rightarrow 0$. From a practical perspective, the computational cost grows inversely with ℓ . Therefore, one would like to use as large an ℓ as possible. However, the proof does not tell us what the largest value for ℓ is at which the results can still be meaningful. Our analysis answers this question by stating that ℓ should at least be smaller than $\min\{W, \ell_c\}$. This might suggest that the solution to the broadening problem is straightforward—simply make ℓ smaller than both W and ℓ_c . However, this is much easier said than done. For most practical applications, the value for ℓ_c is so small that using ℓ values smaller than ℓ_c is impractical. For example, $\ell_c \approx 10\text{ nm}$ for silicon. In 2D, even a $1\text{ }\mu\text{m}$ square specimen would require us solving one million equations. Of course, with recent advances in parallelization and computational power it is routinely possible to solve such large systems of equations on computer clusters. However, recall that the PI's scientific vision involves using PFT computations as investigative tools. This requires the analyst to run a PFT simulation repeatedly to study the effect of different architectural features on the manner in which the crack patterns evolve and affect the toughness. Currently, solving 0.3 million equations takes us 56 hours of CPU time when solving them in parallel on 16 CPU cores. Thus, in summary, our analysis shows that broadening is a major problem, and because of it computational simulations based on the current PFT cannot be used as practical investigative tools.

2.3 Research tasks

We will achieve ***Sro.I*** by carrying out the following two tasks. **Task.1)** Develop a new PFT that will be free of the problem of broadening. **Task.2)** Build the capability in the new PFT to model interfacial fracture.

Task.1 Through our preliminary research we have developed a promising strategy to eliminate the problem of broadening. The primary issue in the current PFT is that stiffness is uniformly degraded in all directions as d increases. We illustrate this situation schematically in Figure 3 (e), where bonds both perpendicular and parallel to the crack are broken. Physically, however, it is only necessary that the bonds perpendicular to the crack are broken, as illustrated, e.g., in Figure 3 (f). We found that the PFT artificially degrading the parallel bonds is the source of the broadening effect. Therefore, we will solve the problem of broadening by developing a new PFT in which the parallel bonds remain intact. We will begin the development of the new PFT by introducing in it information about the crack orientation and using that information to degrade only the bonds that are normal to the crack surface. Specifically, we will begin by making the strain energy term in the energy functional have the more general form $\int_{B_0} \Psi(X, F, \hat{D}, d) d\Omega$, where \hat{D} is a unit vector containing information about the orientation of the crack. If $d = 1$ at some X_c and there is a single crack containing X_c , then $\hat{D}(X_c)$ is interpreted as a direction that is normal to that crack at X_c . Using \hat{D} we will construct Ψ such that the stiffness is only degraded in the direction normal to the crack. Our preliminary calculations show that this strategy is promising for resolving the problem of broadening. We will present an example calculation shortly.

The construction of Ψ may appear challenging. However, it can be simplified by making use of the fact that any proposed Ψ has to satisfy the fundamental principles of material behavior and mechanics. For example, we will reduce the allowable forms of Ψ by requiring that it (P.1) obey the principle of material frame indifference, and (P.2) respect the symmetries of the material. For instance, we found that for an isotropic material Ψ satisfies P.1 and P.2 if it has the reduced form $\Psi(X, \hat{D} \cdot A(U)\hat{D}, \lambda_1, \lambda_2, \lambda_3)$, where U is the positive square root of C , $(\lambda_1, \lambda_2, \lambda_3)$ are the eigenvalues of U , and the tensor valued function $A(U)$ satisfies the condition $A(QUQ^T) = QA(U)Q^T$. For example, in 2D consider $\Psi_d^{\text{NH}} = \mu/2((\lambda_1^2 + \lambda_2^2 - 2) - d(a_1^2\lambda_1^2 + a_2^2\lambda_2^2 - 1))$, where a_1, a_2 are the components of \hat{D} in the eigenvector directions of U . This strain energy density function is a specialization of the reduced form for the case $A(U) = U^2$.

When $d = 0$ everywhere then it reduces to the classical incompressible neo-Hookean material model. If we re-solve the 2D cracked strip problem (see Figure 3 (d)) using Ψ_d^{NH} instead of the previously used $(1-d)^2(\mu/2)(\lambda_1^2 + \lambda_2^2 - 2)$, then we find that if $\ell \ll W$ then at distances of the order of ℓ away from the pre-existing crack $d(\xi) < 2e^{-1/\ell} + O(e^{-2/\ell}) \approx 0$ irrespective of the amount of stretch λ_2 . Thus, with the new Ψ_d^{NH} the broadening effect has vanished.

These are fascinating results. They give us confidence that we are looking in the right direction for solving our research problems and also give us a glimpse of the highly valuable advances that are possible by pursuing the outlined research to its conclusion.

The next step in our strategy is to (**Task.1.i**) verify whether the Ψ_d at hand eliminates broadening in general. (*Case (a)*) If it does then we will move further in this direction and (**Task.1.ii**) extend the Ψ_d to the compressible regime. Following that (**Task.1.iii**) we will linearize the governing equations for small-deformation which should allow us to model fracture of brittle materials without the problem of broadening. (*Case (b)*) If does not, then (**Task.1.bii**) we will experiment with other $A(\mathbf{U})$ to derive a new Ψ_d . Then we will go back to Task.1.i using the new Ψ_d . If we are unable to arrive at a workable Ψ_d by experimenting with different $A(\mathbf{U})$ then (**Task.1.biii**) we will try to further reduce the form of Ψ_d by applying additional constraints on its allowable form. One idea for deriving additional constraints is to enforce the condition that Ψ_d satisfy some type of sufficiency conditions in order for the variational problem involving Ψ_d to be well-posed. By introducing the generalized displacement $\tilde{\mathbf{U}} := (\mathbf{u}, d\hat{\mathbf{D}})$ and the generalized displacement gradient $\tilde{\mathbf{F}} = \nabla_0 \tilde{\mathbf{U}} + \mathbf{I}$ we will try to map our problem to the one discussed in the seminal work of Ball [82]. If we are successful, then we will apply the polyconvexity related sufficiency conditions established in [82] to derive additional constraints on the form of Ψ_d . We will enforce the additional constraints to arrive at a highly refined form of Ψ_d . The highly refined form of Ψ_d should allow us to quickly apply Task.1.i to its different particularizations and arrive at a Ψ_d that is devoid of the problem of broadening.

Following Task.1.iii we will (**Task.1.iv**) numerically implement the new PFT using the same finite element techniques and nonlinear solver algorithms that we used for producing the preliminary results shown in Figure 2. We will then (**Task.1.v**) check that the new PFT's predictions match LEFM results and experimental crack path measurements by performing calculations similar to those shown in Figure 2. Finally, we will (**Task.1.vi**) check that numerical simulations using the new PFT do not exhibit broadening by performing calculations similar to those shown in Figure 3.

Task.2 The fracture of the mineral phase in an SB is expected to be brittle. However, very little is known about the fracture behavior of the interfaces in SBs. Some experimental results suggest that there could be plastic dissipation at the interfaces [41]. However, initially, we will model the interfacial fracture too as being brittle. This is done in order to make the problem tractable, since the proposed approach is new. Eventually, after the successful completion of the current project, we plan on developing PFT for ductile fracture and we will consider then whether a different fracture model for the interfaces would be more appropriate.

In standard PFT the fracture toughness g_c is considered to be a constant (see §2). Our approach for modeling interfacial fracture is as follows. We will allow g_c to vary spatially, such that $g_c = g_c(\mathbf{X})$. To understand how this spatial variation of g_c models interface toughness consider an infinite solid containing a straight interface. We model this interface by setting $g_c = g_I$ over a thickness of $m\ell$ along the straight line denoting the interface. Everywhere else we set $g_c = g_b$, the fracture toughness of the bulk. One would expect the interface's toughness in this case to simply be g_I . However, we find that the connection between $g_c(\mathbf{X})$ and the effective toughness of the interface, g_{int} , could be more nuanced than that. Keeping the initial and final states of the solid stress free, we cleave the solid along its interface into two equal halves. As per PFT, the interface toughness is equal to the smallest amount of work done among all possible cleaving operations in the limit of vanishing ℓ . Carrying out all the calculations we get that, interestingly,

$$g_{int} = g_I (e^\alpha + \tanh(m)) / (e^\alpha \tanh(m) + 1), \quad (3)$$

where $\alpha = \ln(g_b/g_I)$. Therefore, g_{int} lies between g_I and g_b for different values of m . The preliminary interfacial fracture simulations shown in Figure 4 (c) and Figure 5 (d) and (e) were performed using (3).

In order for our approach of modeling interfacial fracture by spatially varying g_c in a piecewise constant manner and setting the value of the interface toughness using (3) to be valid it is necessary to (**Task.2.i**)

show that Eqn. (3) holds for arbitrary 2D solid geometries and arbitrary shapes of interfaces. Though in general the work done during the cleaving cannot be obtained for finite ℓ we found that the problem becomes tractable when $\ell \rightarrow 0$. Thus, we will simplify the problem using the limit $\ell \rightarrow 0$ and determine the relationship between g_{int} and other problem parameters. **Task.2.ii)** This task involves extending the results established through *Task.2.i* to 3D. **Task.2.iii)** In this task we will numerically check that the dependence of g_{int} on problem parameters obtained through *Task.2.i–ii* is correct by numerically simulating crack initiation at interfaces.

3 ***Sro.II:*** Evaluate the predictive potential of the newly developed PFT through experimental comparison

3.1 Identifying the key architectural features in *id*-materials

The new PFT based computational tools developed through the fulfillment of *Sro.I* will be free of the problem of broadening and therefore will be able to model the evolution of complex fracture patterns in realistic *id*-SBs models. As stated in the PI's scientific vision, the goal of developing the new PFT is to use it for performing accurate and robust virtual experiments on *id*-SBs. However, to realize this goal it is important that the new PFT tools are able to correctly capture the salient characteristics of an *id*-material's failure behavior. Therefore, we will evaluate the predictive capability of the developed PFT tools by comparing their results with measurements from fracture tests conducted on a model *id*-SB.

We will use the skeletal elements of the marine sponge *Euplectella aspergillum* (EA), called spicules, as the model *id*-SB in our evaluation [83, 84]. The EA spicules are hair-like fibers that are roughly 10 cm long and 50 μm in diameter and are composed primarily of biogenic silica. They have a tubular, tree-ring type architecture (see Figure 1 (a)). Our preliminary mechanical tests showed that the interfaces were weak. The PI has considerable experience studying structure-property connections in EA spicules [85]. However, the primary reason for selecting EA spicules over other SBs, such as shell or bone, is that their architecture has a good balance between mathematical regularity and complexity. The EA spicules, owing to their axisymmetry, can be described using less than 30 parameters. This will allow us to build the required EA spicule CAD models and complete our evaluation within the allocated time period of the project. At the same time, the spicule's architecture has all of the key features of *id*-materials (brittle layers, many interfaces, 3D architecture). Furthermore, our preliminary mechanical tests show that the EA spicules' failure response is considerably different from that of spicules from a related species that lack the tree-ring architecture (see Figure 4 (b)). This implies that there are interesting architecture-created toughening mechanisms operating in EA spicules. Therefore, the new PFT tools will have to capture non-trivial correlations and mechanisms in order for their predictions to match well with experiments, thus giving us a true measure of their capability.

3.2 Research tasks

The planned comparison will consist of three major tasks: **Task.1)** Build a PFT computational model for the spicule, **Task.2)** Characterize the spicules' failure behavior, and **Task.3)** Compare the measurements to the new PFT tool's predictions.

Task.1 To build a PFT computational model of the spicule we need the following information: spicule architectural parameters, elastic and fracture toughness properties of the spicule's silica, and fracture toughness of the spicule's interfaces. This data will be collected by completing the following subtasks:

Task.1.i) Architecture measurements. The PI has used SEM imaging to measure the silica cylinder thicknesses in the EA spicules as reported in [85]. We will measure the spicule radius, core radius, and silica cylinder thicknesses using the same procedures used in [85] in all spicules that we test in Task.2.

Task.1.ii) Measure fracture toughness and elastic modulus of the spicule's biogenic silica. Although the EA spicules are predominantly composed of silica, it has been shown that many spicules from other sponge species possess a proteinaceous scaffold within their silica [86, 87]. Therefore, we will measure the elastic modulus and toughness of the EA spicules' silica using nanoindentation. The toughness properties of the silica cylinders in the spicules of the sponge *Monorhaphis chuni* have previously been measured using nanoindentation [88, 89]. We will use the same experimental protocol in our work. The spicule's core is roughly 20 μm in diameter, which is a sufficient area for performing the nanoindentation tests. We will

compute the silica's toughness using the classic Lawn-Evans-Marshall model [90, 91]. Nanoindentation will also be used for measuring the silica's reduced elastic modulus, E^* . For that purpose we will follow the procedure described in [92]. The PI has previous experience measuring mechanical properties using nanoindentation [47, 48].

Task.1.iii) *Measure the fracture toughness of spicules' interfaces.* Since the spicules' silica cylinders are both thin and brittle, measuring the fracture toughness, g_I , of the weak interfaces between them is a challenging task. Motivated by the classical fiber push-out test [93], which is used to measure interface toughness in fiber reinforced composites, we have designed the following "cylinder push-out" test for measuring g_I .

One broken spicule segment from each bending test (see Task.2) will be embedded in epoxy and cross-sectioned using a diamond saw to create a 1–3 mm thick slab (see Figure 4 (e)). The exposed spicule cross-section will first be polished, and then a blunt diamond indenter will be used to push against the core. On the opposite side of the slab, all silica cylinders will be mechanically supported (see Figure 4 (e)). This configuration will freeze the relative motion of all weak interfaces except the first one between the core and its adjacent silica cylinder. Thus, the core and the silica cylinders are analogous to the fiber and matrix, respectively, in the fiber push-out test [93].

We will adapt the mechanical testing stage (MTS), which we use to perform the bending tests (Task.2), to perform the cylinder push-out test. During the test we will measure the applied force and indenter displacement. We have made preliminary estimates of the force and displacement ranges needed for this test and found that our modified MTS will be able to perform the cylinder push-out test with 50 nm displacement resolution and 4 μN force resolution.

A typical load-displacement curve from a fiber push-out test performed on a silicon carbide fiber reinforced composite is shown in Figure 4 (f). Initially, the applied force increases linearly with indenter displacement. The abrupt drop in force from P_d to P'_d corresponds to the formation of a crack along the fiber-matrix interface shown schematically in Figure 4 (e). Upon further loading, the applied force again increases until it reaches P_i , at which point the crack begins to propagate along the length of the fiber. If the length of the crack, l_d , at P'_d is large compared to the core radius, r_0 , then the initiation force, P_i , is related to g_I as $P_i = 2\pi\sqrt{r_0^3 g_I E^*}$ [95–97]. Knowing E^* (from Task.1.ii), and r_0 (from Task.1.i), we will compute g_I by measuring P_i in the cylinder push-out test. However, after the test is completed we must verify that $l_d \gg r_0$. We can compute l_d by measuring the stiffness from the force-displacement response before and after crack nucleation, and choosing l_d in a finite element model to match this stiffness ratio. If l_d is not much larger than r_0 , then we will numerically compute the energy release rate for the cylinder push-out test using a finite element model in order to obtain g_I [98].

Task.2 We will characterize the spicules' failure behavior by measuring the load-displacement response of a notched spicule in a three-point bending fracture test. The PI has designed and built a MTS that is capable of performing the fracture tests with 200 nm displacement resolution and 20 μN force resolution. The MTS's design is based on that of an Atomic Force Microscope (AFM). The PI has considerable experience using the AFM for performing mechanical tests [49, 99]. Load-displacement measurements from preliminary bending tests performed on un-notched spicules using the MTS are shown in Figure 4 (b). In the proposed tests, we will cut notches in the spicules in order to match the initial damaged state of the spicules in the experiments with the simulations. Through our preliminary research we were able to successfully create 5–25 μm long notches with a sharpness of approximately 100 nm using focused ion beam milling (see Figure 4 (d)).

Task.3 We have designed the experiments and simulations so that the geometry, internal architecture, initial damage condition, and material properties match as closely as possible. Thus, we can characterize the PFT's predictive capability by whether it is able to reproduce the measured load-displacement curves. A preliminary, 2D model of a spicule (see Figure 4 (c)) produces a load-displacement response that qualitatively matches the jaggedness of the responses from the un-notched bending tests (see Figure 4 (a)). Based on statistics from our initial un-notched bending measurements, we plan on testing 60 spicules harvested from four different EA skeletons.

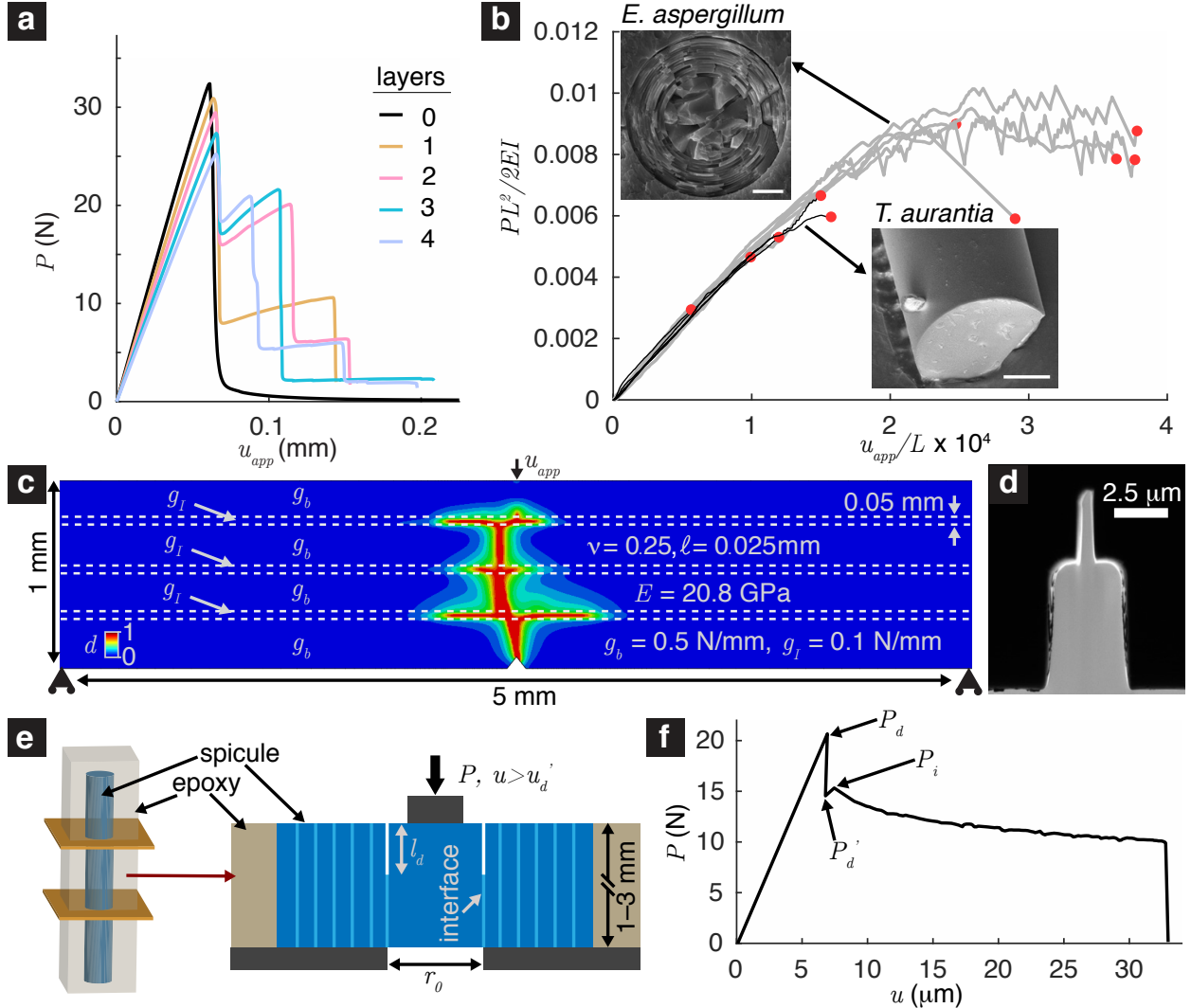


Figure 4: Measurement of the mechanical properties and behavior of spicules. (a) The load-displacement response of a 2D spicule model shown in (c) predicted by the PFT tool for different numbers of interfaces. (b) Dimensionless load-displacement responses of 5 un-notched EA spicules in three-point bending (solid lines). The left inset shows the tree ring architecture of an EA spicule. The dimensionless load-displacement responses of 5 un-notched spicules from a related species (*T. aurantia*) that lack the tree ring architecture (see the right inset) are shown as dashed lines. The scale bars in both insets measure 10 μm . (c) The crack path evolution predicted by the PFT tool for a 2D spicule model loaded in three-point bending. (d) SEM micrograph of a notch cut in a spicule using FIB milling. (e) Configuration of the the proposed cylinder push-out test. A spicule is embedded in epoxy, and cross-sectioned along the orange planes. The silica cylinders from the cross-section are mechanically supported from below and the core is pushed from above (shown in gray). The light blue lines indicate the interfaces between silica cylinders and between the first cylinder and the core. The initial interface crack with length l_d is marked. (f) A typical load-displacement response obtained from a fiber push-out test (data obtained from [94]).

4 *Sro.III: Use the new PFT computational tools to identify new toughening mechanisms in id-materials*

4.1 Identifying toughening mechanisms in materials with wavy interfaces

Wavy interfaces are a prominent architectural motif in *id*-SBs, such as woodpecker beaks (see Figure 5 (b)) and the cranial bones of rams, that are subjected to impact or cyclic loads but must remain intact to perform their mechanical functions [100, 101].

Based on his previous studies of adhesion between wavy surfaces, the PI believes that the wavy interfaces

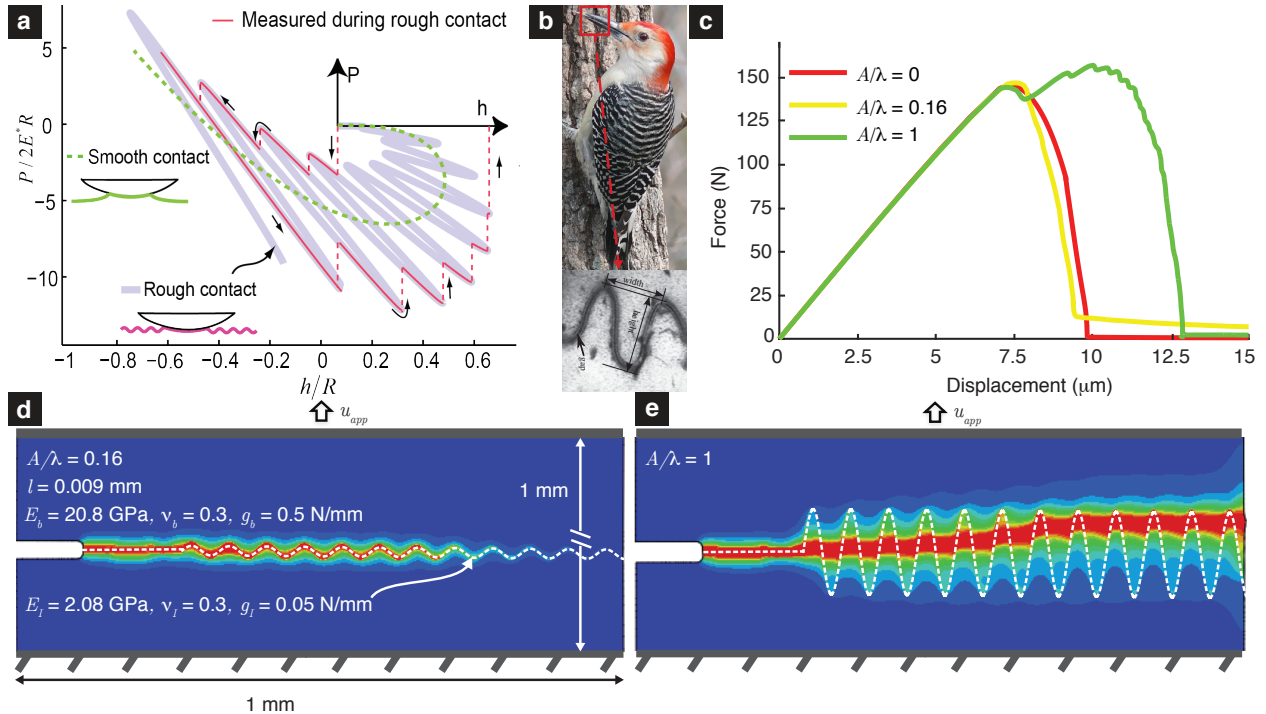


Figure 5: Simulation of fracture of WIs. (a) Load-displacement hysteresis for contact between wavy surfaces. The magenta lines show the series of surface instabilities. (b) Wavy interfaces between keratin scales in the beak of the red bellied woodpecker (photo from [107], micrograph reprinted from [100]). (c) Load-displacement curves for different aspect ratios A/λ of the interface shown in (d-e). (d) Crack propagation along a wavy interface for small A/λ . The interface is shown as a dashed line. (e) Cracks jump out the interface and propagate through the bulk material for large A/λ .

could be a key ingredient for enhancing the toughness of these materials [102–105]. The PI has previously studied the hysteretic load-displacement response that results from adhesive contact between two wavy surfaces [47] (see Figure 5 (a)). He found that this hysteresis can be attributed to a series of surface instabilities (marked with dashed magenta lines in Figure 5 (a)), in which the contact area grows or recedes by a finite amount. Interestingly, the amount of energy lost through this hysteresis is controlled by the amplitude and wavelength of the rough surface. Therefore, even though the interface's intrinsic adhesion energy is constant, the interface's waviness can increase the measured — i.e., the effective — adhesion energy. Similar adhesion energy enhancement has been reported for thin films with adhesive heterogeneities [106]. Motivated by this discovery and the similarities between the mechanics of contact and fracture, the PI proposes to use the PFT tool to search for new toughening mechanisms in materials with wavy interfaces. One of the primary differences between the wavy surface adhesion and wavy interface fracture problems is that in the case of fracture, a crack is not required to travel along the interface as it is in the adhesion problem. Rather, in the fracture problem, the crack can either travel along the interface or propagate through the bulk (see Figure 5 (d)-(e)). The PFT tool is ideally suited to handle this additional level of complexity.

The PI has performed a preliminary study of crack propagation in materials with wavy interfaces using the PFT tool (see Figure 5 (d)-(e)). In these simulations we allowed g_c to vary spatially, so that in most of the solid it had a high value, g_b , and at a predefined wavy interface of finite thickness, it had a low value, g_I . In our preliminary simulations depending on the parameters A/λ and g_I/g_b the failure of the interface displayed very rich mechanics. Here, A and λ are the amplitude and the wavelength of the interface, respectively. For example, we found that at small A/λ the crack always propagated along the interface (see Figure 5 (d)). However, at larger A/λ the crack repeatedly ventured out of the interface into the bulk and then back into the interface through a series of energy dissipating instabilities (see Figure 5 (e)). This lead to substantial toughening in the load-displacement response—i.e., area under the load-displacement curve (see Figure 5 (c)).

4.2 Research tasks

While these results suggest that there may be new toughening mechanisms operating in materials with wavy interfaces, it is not yet understood how toughness varies with the parameters describing the interface's waviness. Further investigation of the relationship between toughness and waviness is motivated by theoretical models that suggest that toughness can be enhanced by increasing the complexity of the interface's undulations [28, 29]. We will achieve ***Sro.III*** by carrying out the following two major tasks. **Task.1)** Perform a parametric study to identify the relationship between effective toughness (i.e., area under the load-displacement curve) and the parameters A/λ , g_I/g_b , and $E\lambda/g_b$. **Task.2)** Using the output of Task.1, construct a simple theoretical mechanics model that captures the key toughening mechanisms operating in materials with wavy interfaces. This model should be able to reproduce the mechanical responses obtained from the parametric study.

Table 1: Project timeline

Task\Year	1	2	3	4	5
<i>Sro.I</i>	T1.i, T1.ii, T1.iii, T1.iv	T1.v, T1.vi, T2.i, T2.ii	T2.ii, T2.iii		
<i>Sro.II</i>	T1.i, T1.ii	T1.ii, T1.iii	T1.iii	T2	T3
<i>Sro.III</i>				T1	T2

5 Broader impacts

5.1 Educational impact through outreach, mentoring, and teaching

The PI believes that everyone should have an opportunity to experience the excitement of science and engineering and has therefore planned a broad range of educational outreach activities. The proposed research has strong links to the subjects of patterns in nature, evolution through natural selection, and bio-inspiration, which generally attract wide public and student interest. Therefore, the PI plans to leverage the research of the proposed project to reach people from a wide variety of backgrounds and excite them about science and engineering. The planned outreach activities will be organized in collaboration with (eo.i) the Sci-Toons initiative and (eo.ii) the SPIRA summer camp at Brown. Activity eo.i has a broad and global focus, whereas activity eo.ii is sharply focused on encouraging high school age girls to pursue higher education in engineering. All outreach activities will be based on the topics, ideas, and results generated from the research component of the project. This strong integration of the educational activities with the research component will make the proposed educational activities more impactful by giving them substance.

The PI has had a productive history of collaboration with the Sci-Toons initiative and the SPIRA program. However, the proposed SPIRA and Sci-Toons activities are all new and unique to the current project. The proposed outreach activities will be kept separate from any other outreach activities that the PI may carry out in collaboration with Sci-Toons and SPIRA. The PI's history of collaboration with Sci-Toons and SPIRA will add to the quality of the proposed activities. This is because the PI will be able to draw on his past experiences of working with the Sci-Toons and SPIRA staff and will be able to leverage the partnerships he has developed with them over the years.

Collaboration with the Sci-Toons initiative The Science Cartoons (Sci-Toons) initiative is a new strategy for communicating scientific research and concepts to a broad audience via storytelling, animation, high-quality multimedia and art. The initiative, part of broader impacts and education activities at Brown University's Science Center, engages STEM students, non-STEM students and faculty to create science animation videos that conceptualize and communicate science in an engaging and compelling manner to a broad range of audiences. The PI and his students will collaborate with the SciToons Creation Group (SCG), led by Dr. Oludurotimi Adetunji, Associate Dean for Undergraduate Research and Inclusive Science; and Executive Producer of the Brown University SciToons Initiative. The SCG consists of both STEM and non-STEM students, STEM domain content experts, voice over artists and animators.

The Sci-Toons program's broader impacts goal of fostering greater understanding and appreciation of science in the general public is advanced by meshing communication and science, skills and interests of

STEM and non-STEM majors. Four students, the PI and Dr. Adetunji are currently collaborating to produce a Sci-Toon animation that, through “jargon-free” language and storytelling, communicates the importance and impact of the results from the PI’s recent publication [85] to a non-scientific audience. As part of the proposed project, the PI, in collaboration with SCG, will create one video per academic year for the next five years. The collaboration through this proposal will begin in Fall 2017. The videos will focus on the latest results from the research wing of the project. They will end by highlighting that the vast majority of the nature’s designs are still unknown, and we will try to excite the viewers about the immense possibilities that the discovery of such designs would create for science and engineering. Funds to support the PI’s future collaboration with the Sci-Toons initiative are requested as part of the budget (see Budget Justification). *Evaluation:* The viewing impacts of Sci-Toons videos are gauged by monitoring the number and geographic distribution of views the videos generate using google analytics data. Prior Sci-Toons videos have been viewed in over 180 countries. Examples of completed Sci-Toons can be viewed on the Sci-Toons’ YouTube channel.

In addition to the Sci-Toons YouTube channel and a dedicated website, the Sci-Toons videos are distributed via a variety of social media platforms, such as Twitter (@Sci_Toons) and Facebook. The Sci-Toons videos will also be posted on the PI’s lab website. The website will be set up so that viewers can post comments and questions about the videos. The PI and his students will host a monthly virtual discussion group on Google Hangouts and address the posted comments and questions live. The PI will use the Sci-Toons videos in the undergraduate courses he teaches at Brown, such as Advanced Engineering Mechanics (ENGN 1370) and Advanced Engineering Optimization (ENGN 1950), which share the elements of solid and structural mechanics, and optimization principles with the topics that will be highlighted in the videos. The PI will also encourage his colleagues at Brown and other universities to use the videos in introductory engineering courses and in courses related to mechanics and optimization. *Evaluation:* The videos’ impact and utility in the classroom will be gauged by using the end of course student feedback form.

Collaboration with SPIRA SPIRA is a four week camp hosted at Brown every summer for high school age girls to explore engineering. For the past three years, the PI and his students have been collaborating with SPIRA in order to encourage young women to pursue education in STEM fields by exposing them to interesting applications of engineering. The camp is free to those who attend and often attracts students from underrepresented minorities. Over the course of the proposed project, every summer, the PI and the student associated with the project will design and organize talks, workshops and competitions for the SPIRA participants. These activities will be tailored to make the participants aware of the wide range of exciting opportunities that are only recently becoming available to engineers, and through this awareness attract them to science and engineering. *Talks:* Some of the past talks have been “Better materials through micro-scale mechanical design” and “Bio-inspired engineering: why should we listen to nature.” These talks were focused on the importance of bio-inspired materials to the future of mechanical engineering. Future talks will have a similar focus. The new results from the research component of the project will be used to enhance the quality of the talks. Following the talk, the students will be given a tour of PI’s lab during which the presented research will be further explained using physical examples and practical demonstrations. *Lab tour and workshop:* During the lab tour, the PI and his students will also explain the operating principles behind the different lab equipment. Last year’s workshop was titled, “Hidden genius: a closer look at nature’s architecture.” In it, the participants examined spicules from the EA sponge as well as other biomaterials. Pictures from last year’s lab tour and workshop are shown in Figure 6. The first workshop that will be held as part of the project is tentatively titled, “Engineering Principles in Nature”. In it, the PI’s team and the participants will discuss the size, form, and function relationships in SBs, such as mammalian bones, eggshells, gecko’s feet and the venus fly trap. *Competition:* The competitions will give the participants an opportunity to learn through hands-on practice and experimentation. A competition under development for this project’s SPIRA activities is tentatively titled “Soft landing: better materials for tomorrow’s helmets and cars”. In the competition the participants will be asked to construct a structure for cushioning the fall of a dropped egg by taking inspiration from nature. The student teams will be supplied with various materials and given access to the microscope in the PI’s lab. Funds to organize this new competition in collaboration with SPIRA are requested as part of the budget (see Budget Justification). *Evaluation:* The effectiveness of the planned SPIRA lectures, tutorials, and competitions will be gauged using exit interviews. The students’ feedback will also be solicited by encouraging them to post comments

and suggestions on the SPIRA section of the PI's website.

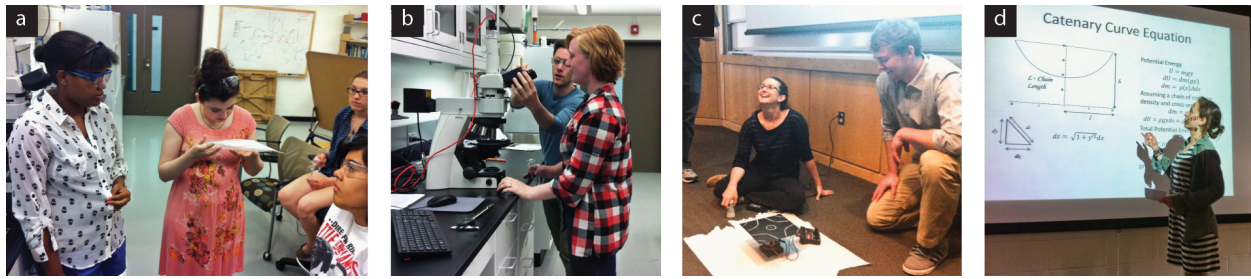


Figure 6: (a)–(b) SPIRA students and (c)–(d) undergraduates From the PI's courses taking part in activities that were designed using the output from the PI's research program. The activities included several examples of how mechanics of materials research is enabling engineers to solve critical societal problems.

Mentoring of Brown graduate and undergraduate students The PI is currently advising four Ph.D. students (Michael Monn, Weilin Deng, Kaushik Vijaykumar, and Wenqiang Fang), one master's student (Jianzhe Yang), and one undergraduate honors thesis student (Christopher Owen-Elia). The PI recently graduated two master's students (Jarod Ferreira and Tianyang Zhang) and has directed six undergraduate research projects. Apart from two of the Ph.D. students, all of the other students' research topics are related to the proposed research. This demonstrates the PI's commitment, focus, and passion for the proposed research. Research performed by the PI's Ph.D. students, principally Michael, and Kaushik, generated the preliminary results presented in this proposal. Funds to support one new Ph.D. student are requested as part of the Budget (see Budget Justification).

Like the PI's other students, the new Ph.D. student will be provided with ample research guidance and support; the PI encourages one-on-one technical discussions and maintains an open door policy. Additionally, they will also be trained in the skills of scientific writing, oral presentation, and teaching techniques, which are necessary for future success. This will be achieved through the PI actively co-authoring research papers with the student and encouraging them to give oral presentations in lab group meetings, to serve as Teaching Assistants in the courses taught by the PI, and to attend technical conferences on mechanics of materials and structures, such as the annual technical meetings of the Society of Engineering Science and American Society of Mechanical Engineers, and the International Congress of Theoretical and Applied Mechanics. The PI tailors his guidance with an eye on his students' career development and their future after graduation. Close to graduation, the PI takes active part in helping his students get placed and integrated into the wider scientific community or industry.

6 Results from prior NSF support

CMMI-1562656: "Emergence of New Properties at the Large-Scale on Elastic Surfaces due to Small-Scale Adhesion and Waviness," \$375,000, 03/01/2016 – 02/28/2019. **Intellectual merit** The objective of this research is to understand how contact interactions between two surfaces at the micro-scale manifest as friction-like behavior at the macro-scale. Specifically, we relate friction at the macro-scale to dissipative mechanisms acting at the micro-scale that are activated by both adhesion and surface roughness. Through a synergistic combination of theoretical analysis, computer modeling, and experiments we will develop a rigorous mechanical theory governing the relationship between friction, adhesion, and surface roughness. A better understanding of this relationship could lead to advances in pick-and-place technology, MEMS, and biomimetic climbing robots. No publications have been produced under this award so far. As per the Data Management Plan for this award, computer code, experimental data, and theoretical results will be made available through the Dropbox cloud storage system following publication. **Broader impacts** Three graduate students (Wenqiang Fang, Weilin Deng, Jarod Ferreira), and one undergraduate student (Christopher Owen-Elia) have worked on projects supported by this award. A masters thesis titled "Adhesive contact experiments with non-linear model fitting" has been completed by Jarod Ferreira under the supervision of the PI. Additionally, one journal article titled "Depth-dependent hysteresis in adhesive elastic contacts of large surface roughness" is currently in preparation, and is co-authored by Weilin Deng and the PI.